

## Fully relativistic calculation of the two-photon momentum distribution for positron annihilation in tungsten

G. J. Rozing and P. E. Mijnarends

*Netherlands Energy Research Foundation ECN, 1755 ZG Petten, The Netherlands*

R. Benedek

*Materials Science Division, Argonne National Laboratory, Argonne, Illinois 60439*

(Received 26 June 1990)

A method is described for the calculation of the two-photon momentum distribution for positron annihilation, which employs the eigenvectors from a fully relativistic band-structure calculation. Although the usual nonrelativistic positron-electron overlap integral is used, effects of spin-orbit coupling on the two-photon momentum distribution are introduced via the band structure and the wave functions. The method is implemented for the relativistic linearized augmented-plane-wave method and applied to tungsten.

### I. INTRODUCTION

The measurement of the angular correlation of annihilation radiation in two dimensions (2D-ACAR) is a valuable technique to obtain information about the electronic structure of solids. With this method the Fermi surface of a great number of metals and intermetallic compounds has been studied.<sup>1</sup> In general, the interpretation of 2D-ACAR experiments is facilitated by a computation of the momentum distribution of the two photons emitted in the annihilation process. Integration of this calculated two-photon ( $2\gamma$ ) momentum distribution along a specified direction in momentum space yields a two-dimensional distribution that can be compared directly with the measured 2D angular correlation.

In recent years attention has focused on compounds containing atoms from the rare-earth and actinide series. The more or less localized character of the  $f$  electron introduces entirely new physical properties, which express themselves most clearly in the class of heavy-fermion systems.<sup>2</sup> Calculations of the band structure and the two-photon ( $2\gamma$ ) momentum distribution of these solids in general require a fully relativistic formalism involving the eigenvectors of the full Dirac Hamiltonian. The cross section for two-photon annihilation has been derived in several textbooks on quantum electrodynamics. However, the matrix, which couples positron and electron, was only obtained explicitly in the nonrelativistic limit.<sup>3</sup> Devanathan and Iyakutti computed the  $2\gamma$  momentum distribution employing this matrix to couple wave functions that were obtained from the relativistic augmented-plane-wave (RAPW) method.<sup>4</sup> However, as far as we know, to this date no numerical calculations of a  $2\gamma$  momentum distribution have been performed using fully relativistic wave functions (possibly for this reason very few 2D-ACAR measurements on high- $Z$  materials have been reported).

Section II discusses the form of the relativistic wave

functions and the coupling of the positron and electron wave functions in the two-photon annihilation process. We derive the RAPW expressions for the  $2\gamma$  momentum distribution in Sec. III. This derivation differs from that in Ref. 4 only in the treatment of the positron wave function. Section IV discusses how these expressions can be modified to make them suitable for use of the relativistic linearized augmented-plane-wave (RLAPW) method, whereafter the results are presented of numerical calculations on tungsten. For the first relativistic calculation of a  $2\gamma$  momentum distribution tungsten was chosen as the model material because its band structure shows prominent effects of the spin-orbit interaction.<sup>5</sup> Finally, Sec. V summarizes the conclusions of this work.

### II. COUPLING OF RELATIVISTIC PARTICLES

In the independent-particle model the two-photon momentum distribution  $\rho_{2\gamma}$  at momentum  $\mathbf{p}$  is given by<sup>6</sup>

$$\rho_{2\gamma}(\mathbf{p}) = \sum_{\mathbf{k}, n} f_n(\mathbf{k}) |A_n(\mathbf{p}, \mathbf{k})|^2, \quad (1)$$

with the nonrelativistic overlap integral

$$A_n(\mathbf{p}, \mathbf{k}) = \int_V e^{-i\mathbf{p}\cdot\mathbf{r}} \psi_+(\mathbf{r}) \psi_n(\mathbf{k}, \mathbf{r}) d\mathbf{r}. \quad (2)$$

Here  $\psi_n(\mathbf{k}, \mathbf{r})$  and  $\psi_+(\mathbf{r})$  represent the (single-component) wave functions of the annihilated electron with wave vector  $\mathbf{k}$  and band index  $n$ , and the positron in its ground state  $\mathbf{k}=\mathbf{0}$ , respectively. The Fermi-Dirac distribution function  $f_n(\mathbf{k})$  determines the occupation of the electron states. The integration extends over the entire crystal of volume  $V$ . The spin indices have been omitted, but Eqs. (1) and (2) imply opposite positron and electron spins as only a spin-singlet pair can annihilate into two photons. In the nonrelativistic approximation and zero magnetic field the spatial part of the wave functions is independent of the spin and therefore both allowed spin singlets give rise to the same expression.

For solids containing high- $Z$  atoms, the kinetic-energy term in the Schrödinger equation becomes large, which results in strong oscillations of the wave function. Hence, the Schrödinger equation should be replaced by the relativistic Dirac equation. Approximations to the Dirac equation essentially leave out the spin-orbit coupling and neglect the small components of the wave function. These semirelativistic methods work well for solids containing atoms with  $Z \leq 60$ , say, but for higher  $Z$  a fully relativistic approach is required. In addition, the use of the full Dirac equation allows one to concentrate on the potential as being the major approximation. Until recently the efforts involved in this approach were considerable, but with the generalization of the linearized methods to full relativity<sup>7</sup> numerical band-structure calculations have become manageable nowadays even for complex crystal structures.

In a fully relativistic treatment, the particles are represented by four-component wave functions. The wave function of a free electron with wave vector  $\mathbf{k}$  is

$$\psi_m(\mathbf{k}, \mathbf{r}) = N(k) \begin{pmatrix} \chi(m) \\ \frac{\boldsymbol{\sigma} \cdot \mathbf{k}}{1+k^0} \chi(m) \end{pmatrix} e^{i\mathbf{k} \cdot \mathbf{r}}, \quad (3)$$

where the spinor

$$\chi(\tfrac{1}{2}) = \begin{pmatrix} 1 \\ 0 \end{pmatrix} \text{ and } \chi(-\tfrac{1}{2}) = \begin{pmatrix} 0 \\ 1 \end{pmatrix}.$$

The matrices  $\sigma_x$ ,  $\sigma_y$ , and  $\sigma_z$  are the well-known Pauli  $2 \times 2$  spin matrices. The normalization constant  $N(k) = [(1+k^0)/2k^0]^{1/2}$ , where  $k^0 = (1+k^2)^{1/2}$ , and  $k = |\mathbf{k}|$  is expressed in relativistic units (a transformation to atomic units replaces  $k$  by  $2k/c$ , where  $c$  is the speed of light). This normalizes the wave function to one particle per unit volume. The index  $m$  in Eq. (3) refers to wave functions with spin up or spin down only in the nonrelativistic limit, where the lower spinor vanishes and the upper one reduces to the nonrelativistic wave function with spin included. From Eq. (3) it can be seen that the spatial and spin-dependent parts of a relativistic plane wave can still be separated. In an external potential, on the other hand, each of the four components is a different function of  $\mathbf{r}$  due to spin-orbit coupling.

The expression for the positron wave function can be obtained from its electron counterpart by application of the charge-conjugation operator<sup>8</sup>

$$\gamma_2 K = \begin{pmatrix} 0 & 0 & 0 & -1 \\ 0 & 0 & 1 & 0 \\ 0 & 1 & 0 & 0 \\ -1 & 0 & 0 & 0 \end{pmatrix} K,$$

with  $K$  denoting the operator of complex conjugation. Charge conjugation of Eq. (3) yields the positron wave function

$$\psi_{+,m}(\mathbf{k}, \mathbf{r}) = N(k) S_{-m} \begin{pmatrix} \frac{\boldsymbol{\sigma} \cdot \mathbf{k}}{1+k^0} \chi(-m) \\ \chi(-m) \end{pmatrix} e^{-i\mathbf{k} \cdot \mathbf{r}} \quad (4)$$

( $S_m$  is the sign of  $m$ ).

The coupling between the annihilating relativistic particles should be represented by a properly relativistic expression for the overlap integral  $A_n(\mathbf{p}, \mathbf{k})$ . In most calculations of the cross section for  $2\gamma$  annihilation free particles are considered with vanishing velocities.<sup>3</sup> It can be shown that in that case the coupling is established by the Dirac matrix

$$\gamma_5 = \begin{pmatrix} 0 & 0 & -1 & 0 \\ 0 & 0 & 0 & -1 \\ -1 & 0 & 0 & 0 \\ 0 & -1 & 0 & 0 \end{pmatrix}$$

(both the coupling matrix  $\gamma_5$  and the charge-conjugation matrix  $\gamma_2 K$  are defined according to Ref. 8, and differ from those in Ref. 3 by factors  $-i$  and  $i$ , respectively), which implicitly assures singlet annihilation for these particles. Although in the present problem we are not dealing with free particles with zero velocities but with relativistic particles moving in a crystal potential, we shall nevertheless use the  $\gamma_5$  matrix to couple the positron and the electron. For a thermalized positron with  $\mathbf{k} = 0$  the overlap integral then becomes

$$A_n(\mathbf{p}, \mathbf{k}) = \int_V d\mathbf{r} e^{-i\mathbf{p} \cdot \mathbf{r}} [\psi_+(\mathbf{r})]^\dagger \gamma_5 \psi_n(\mathbf{k}, \mathbf{r}). \quad (5)$$

The large components of the positron and electron spinors couple to each other and so do the small components. In the laboratory system the contribution from the latter vanishes in the free-particle case due to the positron wave vector being zero. In a solid, on the other hand, the repulsion of the atomic nuclei reduces the positron density in the core region of the atoms, where the potential is strong. Therefore, the upper positron components can be neglected in solids as well, which is supported by calculations of Iyakutti and Devanathan.<sup>9</sup> Hence, only the product of the large components survives the coupling by the  $\gamma_5$  matrix in  $A_n(\mathbf{p}, \mathbf{k})$ . In spite of this, the small components of the electron wave function affect the results implicitly through the normalization.

In zero magnetic field, two eigenstates correspond to each eigenvalue as long as the crystallographic point group has an inversion center. These states are related to each other by the combined operations of time reversal and parity, which is equivalent to spin degeneracy in the nonrelativistic limit.<sup>10</sup> In Eq. (1) the overlap integrals of all four combinations of degenerate electron and positron states have to be included.

Although Eq. (5) is a nonrelativistic approximation, together with Eq. (1) it enables us to calculate the  $2\gamma$  momentum distribution corresponding to a fully relativistic band structure. The Fermi surface causes discontinuities in the momentum distribution through the Fermi-Dirac distribution function; hence, the position of these discontinuities reflects the fully relativistic Fermi surface. The overlap integral may to some extent be influenced by the nonrelativistic nature of Eq. (5). However, as the square of the overlap integral is a relatively smooth function of momentum its lack of relativistic invariance will

not affect the position of the Fermi-surface discontinuities.

### III. THE RAPW OVERLAP INTEGRAL

In this section the RAPW expressions for the wave functions will be substituted into Eq. (5). The band index  $n$  will be omitted for clarity. The RAPW method has been discussed extensively by Loucks<sup>11</sup> and his notation is followed here as much as possible.

As usual, the muffin-tin form for the crystal potential is adopted, which spherically averages the potential at the atomic sites. The electron wave function can then be written as a linear combination of relativistic plane waves [cf. Eq. (3)], augmented inside the muffin-tin spheres with the solutions of the Dirac equation for a spherically symmetric potential. These solutions are equal to the numerical solutions of the radial Dirac equations multiplied by the spin angular functions

$$\chi_{\kappa}^{\mu}(\hat{\rho}) = \sum_m C(l\frac{1}{2}j; \mu - m, m) Y_{l\mu - m}(\hat{\rho}) \chi(m). \quad (6)$$

Here,  $C(l\frac{1}{2}j; \mu - m, m)$  are the Clebsch-Gordan coefficients and  $Y_{l\mu - m}$  complex spherical harmonics.<sup>8</sup> The quantum numbers for each  $l \geq 0$  are  $\kappa = l, j = l - \frac{1}{2} (l \neq 0)$ , and  $\kappa = -l - 1, j = l + \frac{1}{2}$ , with  $\mu = -j, -j + 1, \dots, j - 1, j$ . The augmentation process yields basis functions inside the spheres which are formed by a superposition of these solutions for all  $\kappa$  and  $\mu$ . The appropriate coefficients are found by matching the large components of all terms in the summation to the Rayleigh expansion of the plane wave on the surface of the sphere (see Ref. 11).

For the full electron wave function in the interstitial region we have

$$\psi(\mathbf{k}, \mathbf{r}) = V^{-1/2} \sum_{\mathbf{G}, m} a_{\mathbf{G}m}(\mathbf{k}) N(k_{\mathbf{G}}) \left[ \begin{array}{c} \chi(m) \\ \frac{\boldsymbol{\sigma} \cdot \mathbf{k}_{\mathbf{G}}}{1 + k_{\mathbf{G}}^0} \chi(m) \end{array} \right] e^{i\mathbf{k}_{\mathbf{G}} \cdot \mathbf{r}}, \quad (7)$$

where  $\mathbf{k}_{\mathbf{G}} = \mathbf{k} + \mathbf{G}$ . The RAPW expansion coefficients  $a_{\mathbf{G}m}(\mathbf{k})$ , labeled by reciprocal-lattice vector  $\mathbf{G}$  and spin index  $m$ , are to be determined in a band-structure calculation. Let  $\mathbf{R}_n$  denote a direct-lattice vector,  $\mathbf{R}_v$  the position of the  $v$ th atom in the unit cell, and  $r_v$  the radius of the  $v$ th muffin-tin sphere. Then, with  $\mathbf{r} = \mathbf{R}_n + \mathbf{R}_v + \boldsymbol{\rho}$  and  $\rho < r_v$ , the angular momentum representation of the electron wave function in the  $v$ th sphere yields

$$\psi(\mathbf{k}, \mathbf{r}) = 4\pi V^{-1/2} e^{i\mathbf{k} \cdot (\mathbf{R}_n + \mathbf{R}_v)} \sum_{\kappa\mu} i^l A_{\kappa\mu}^v(\mathbf{k}) \left[ \begin{array}{c} g_{\kappa}^v(\rho) \chi_{\kappa}^{\mu}(\hat{\rho}) \\ i f_{\kappa}^v(\rho) \chi_{\kappa}^{\mu - \kappa}(\hat{\rho}) \end{array} \right], \quad (8)$$

where  $g_{\kappa}$  and  $f_{\kappa}$  are the large and small components of the solution of the radial Dirac equation. The coefficients  $A_{\kappa\mu}^v$  are

$$A_{\kappa\mu}^v(\mathbf{k}) = \sum_{\mathbf{G}} N(k_{\mathbf{G}}) \frac{j_l(k_{\mathbf{G}} r_v)}{g_{\kappa}(r_v)} e^{i\mathbf{G} \cdot \mathbf{r}_v} \\ \times \sum_m a_{\mathbf{G}m}(\mathbf{k}) C(l\frac{1}{2}j; \mu - m, m) Y_{l\mu - m}^*(\hat{\mathbf{k}}_{\mathbf{G}}), \quad (9)$$

where  $j_l$  is the spherical Bessel function of order  $l$ .

The positron wave function is obtained from the electron wave function by charge conjugation. In the interstitial region the wave function of the positron in its ground state at  $\mathbf{k} = \mathbf{0}$  becomes

$$\psi_+(\mathbf{r}) = V^{-1/2} \sum_{\mathbf{G}, m} c_{\mathbf{G}, -m}^* S_m N(G) \left[ \begin{array}{c} \frac{\boldsymbol{\sigma} \cdot \mathbf{G}}{1 + G^0} \chi(m) \\ \chi(m) \end{array} \right] e^{-i\mathbf{G} \cdot \mathbf{r}}, \quad (10)$$

with RAPW expansion coefficients  $c_{\mathbf{G}m}$ . Inside the  $v$ th muffin-tin sphere the angular momentum decomposed positron wave function is (see also Ref. 8, p. 160)

$$\psi_+(\mathbf{r}) = 4\pi V^{-1/2} \sum_{\kappa\mu} (-i)^l C_{\kappa\mu}^v \left[ \begin{array}{c} -i f_{\kappa+}^v(\rho) \chi_{\kappa}^{\mu - \kappa}(\hat{\rho}) \\ g_{\kappa+}^v(\rho) \chi_{\kappa}^{\mu}(\hat{\rho}) \end{array} \right], \quad (11)$$

where, similar to Eq. (9),

$$C_{\kappa\mu}^v = \sum_{\mathbf{G}} N(G) \frac{j_l(G r_v)}{g_{\kappa+}(r_v)} e^{-i\mathbf{G} \cdot \mathbf{R}_v} \\ \times \sum_m c_{\mathbf{G}, -m}^* S_m C(l\frac{1}{2}j; \mu - m, m) Y_{l\mu - m}^*(\hat{\mathbf{G}}). \quad (12)$$

Please note that the treatment of the positron has been fully relativistic up until now.

The integration in Eq. (5) for the overlap integral separates naturally into a contribution from the spheres and an interstitial part

$$A(\mathbf{p}, \mathbf{k}) = A^{(\text{sph})}(\mathbf{p}, \mathbf{k}) + A^{(\text{int})}(\mathbf{p}, \mathbf{k}). \quad (13)$$

Substitution of Eqs. (8) and (11) for the electron and positron wave functions, respectively, into Eq. (5) and restriction of the integration to the spheres gives

$$A^{(\text{sph})}(\mathbf{p}, \mathbf{k}) = -\frac{(4\pi)^2}{\tau} \delta_{\mathbf{p} - \mathbf{k}, \mathbf{K}} \\ \times \sum_{\kappa\mu} \sum_{\kappa'\mu'} i^{l+l'} \sum_v e^{-i\mathbf{K} \cdot \mathbf{R}_v} A_{\kappa\mu}^v(\mathbf{k}) \\ \times C_{\kappa'\mu'}^{v*} I_{\kappa\mu\kappa'\mu'}^v(\mathbf{p}), \quad (14)$$

where  $\tau$  is the unit-cell volume and  $\mathbf{K}$  the reciprocal-lattice vector that reduces the momentum  $\mathbf{p}$  to the corresponding electron wave vector  $\mathbf{k}$  in the first Brillouin zone. The factors  $I_{\kappa\mu\kappa'\mu'}^v$  denote the integrations over the  $v$ th sphere,

$$I_{\kappa\mu\kappa'\mu'}^\nu(\mathbf{p}) = \int_{\nu} e^{-i\mathbf{p}\cdot\rho} \{g_{\kappa}^\nu(\rho)g_{\kappa'}^\nu(\rho)[\chi_{\kappa}^{\mu'}(\hat{\rho})]^\dagger \chi_{\kappa}^{\mu}(\hat{\rho}) - f_{\kappa}^\nu(\rho)f_{\kappa'}^\nu(\rho) \times [\chi_{-\kappa}^{\mu'}(\hat{\rho})]^\dagger \chi_{-\kappa}^{\mu}(\hat{\rho})\} d\rho. \quad (15)$$

Using the Rayleigh expansion for the plane wave, this integral can be factorized into radial and angular parts. At this point it is convenient to use the fact that the small components of the positron wave function are negligibly small, i.e.,  $f_{\kappa}^\nu \ll g_{\kappa}^\nu$ . The derivation then proceeds in a

manner similar to the nonrelativistic APW formalism.<sup>12</sup> A second approximation concerns the almost spherically symmetric nature of the positron wave function inside the muffin-tin spheres. In Eq. (11) all terms with  $l \neq 0$  ( $\kappa \neq -1$ ) may be neglected with little loss of accuracy. The orthonormality of the spherical harmonics then simplifies the angular parts of the integrals substantially. With the radial integrals

$$T_{\kappa}^\nu[p, E(\mathbf{k}), E_+] = \int_0^{r_\nu} \rho^2 j_l(p\rho) g_{\kappa}^\nu(\rho) g_{-\nu-1, +}^\nu(\rho) d\rho, \quad (16)$$

the contribution of the spheres becomes

$$A^{(\text{sph})}(\mathbf{p}, \mathbf{k}) = -\frac{(4\pi)^2}{\tau} \delta_{\mathbf{p}-\mathbf{k}, \mathbf{K}} \sum_{\nu} e^{-i\mathbf{K}\cdot\mathbf{R}_\nu} \sum_{\mu'=\pm\frac{1}{2}} (4\pi)^{1/2} C_{-1\mu'}^{\nu*} \sum_{\kappa\mu} C(l\frac{1}{2}j; \mu-\mu', \mu') Y_{l\mu-\mu'}(\hat{\mathbf{p}}) A_{\kappa\mu}^\nu(\mathbf{k}) T_{\kappa}^\nu[p, E(\mathbf{k}), E_+]. \quad (17)$$

Also, the expressions for the wave functions in the interstitial region for the electron (7) and for the positron (10) are substituted into Eq. (5). Limiting the integration to the interstitial region yields

$$A^{(\text{int})}(\mathbf{p}, \mathbf{k}) = -V^{-1} \sum_{Gm} \sum_{G'm'} a_{Gm}(\mathbf{k}) c_{G', -m'} S_m N(k_G) N(G') I(\mathbf{p}-\mathbf{k}_G - \mathbf{G}') \left[ \delta_{m', m} + \chi^\dagger(m') \frac{\boldsymbol{\sigma} \cdot \mathbf{G}' \boldsymbol{\sigma} \cdot \mathbf{k}_G}{(1+\mathbf{G}'^0)(1+k_G^0)} \chi(m) \right], \quad (18)$$

where  $I$  denotes the integral

$$I(\mathbf{p}-\mathbf{k}_G - \mathbf{G}') = \int_{\text{int}} e^{-i(\mathbf{p}-\mathbf{k}_G - \mathbf{G}')\cdot\mathbf{r}} d\mathbf{r}. \quad (19)$$

In general, due to the convergence of the electron wave functions  $k_G/(1+k_G^0) \approx k_G \ll 1$  for all non-negligible RAPW expansion coefficients. Since this is true *a fortiori* for the positron the second term between the large parentheses in Eq. (18) can be neglected. The integral of Eq. (19) is solved in the usual way by first extending the integration over the whole crystal and then subtracting the contribution from the spheres, which results in the final expression for the interstitial contribution

$$A^{(\text{int})}(\mathbf{p}, \mathbf{k}) = -\delta_{\mathbf{p}-\mathbf{k}, \mathbf{K}} \sum_{Gm} a_{Gm}(\mathbf{k}) N(k_G) S_m X_m(\mathbf{K}-\mathbf{G}). \quad (20)$$

If  $\Omega_\nu$  is the volume of the  $\nu$ th sphere,

$$X_m(\mathbf{K}-\mathbf{G}) = \sum_{G'} c_{G', -m} \left[ \delta_{\mathbf{K}-\mathbf{G}, \mathbf{G}'} - \sum_{\nu} \frac{\Omega_\nu}{\tau} e^{-i(\mathbf{K}-\mathbf{G}-\mathbf{G}')\cdot\mathbf{R}_\nu} \times \frac{3j_1(|\mathbf{K}-\mathbf{G}-\mathbf{G}'|r_\nu)}{|\mathbf{K}-\mathbf{G}-\mathbf{G}'|r_\nu} \right]. \quad (21)$$

This expression does not depend on  $\mathbf{p}$  and  $\mathbf{k}$ , hence it can be conveniently tabulated for all  $\mathbf{K}-\mathbf{G}$ . Note that the full plane-wave expansion of the positron wave function

is retained in the interstitial region. Devanathan and Iyakutti<sup>4</sup> assume a constant positron wave function in that region.

As mentioned before, in zero magnetic field or moment and in the presence of an inversion center each electron or positron eigenvalue is doubly degenerate. The second eigenvector of this pair of states is obtained from the first by the combined operation of time reversal and parity. The operator is<sup>8</sup>

$$i\gamma_4\gamma_3\gamma_1K = \begin{pmatrix} 0 & i & 0 & 0 \\ -i & 0 & 0 & 0 \\ 0 & 0 & 0 & -i \\ 0 & 0 & i & 0 \end{pmatrix},$$

and, when applied to the calculated wave functions before substitution into Eq. (5), yields equations for  $A(\mathbf{p}, \mathbf{k})$  similar to the ones in this section. The square of each of these overlap integrals must be included in the summation in Eq. (1) to yield the total momentum density.

#### IV. NUMERICAL CALCULATIONS FOR TUNGSTEN

For practical calculations of the band structure and the eigenvectors we adopt the relativistic linearized augmented-plane-wave (RLAPW) method.<sup>13</sup> The equations for the  $2\gamma$  momentum distribution derived in Sec. III are easily extended to the linearized version. This leaves the interstitial contribution to the overlap integral, Eq. (20), unchanged. Inside the muffin-tin spheres the radial solutions of the Dirac equation ( $g_\kappa, f_\kappa$ ) are evaluated

at a fixed energy. The price to be paid consists of the inclusion of extra terms, which contain the energy derivatives ( $\dot{g}_\kappa, \dot{f}_\kappa$ ). This yields for the electron

$$\psi(\mathbf{k}, \mathbf{r}) = 4\pi V^{-1/2} e^{i\mathbf{k} \cdot (\mathbf{R}_n + \mathbf{R}_v)} \times \sum_{\kappa\mu} i^l \left[ B_{\kappa\mu}^v(\mathbf{k}) \begin{pmatrix} g_\kappa^v(\rho) \chi_\kappa^\mu(\hat{\rho}) \\ i f_\kappa^v(\rho) \chi_{-\kappa}^\mu(\hat{\rho}) \end{pmatrix} + D_{\kappa\mu}^v(\mathbf{k}) \begin{pmatrix} \dot{g}_\kappa^v(\rho) \chi_\kappa^\mu(\hat{\rho}) \\ i \dot{f}_\kappa^v(\rho) \chi_{-\kappa}^\mu(\hat{\rho}) \end{pmatrix} \right]. \quad (22)$$

The coefficients  $B_{\kappa\mu}^v$  and  $D_{\kappa\mu}^v$  are obtained in a way similar to  $A_{\kappa\mu}^v$  in Eq. (8) by matching the upper components of the RLAPW basis functions on the surface of the spheres. The contribution of the spheres to the overlap integral now involves four types of radial integrals, which are independent of the energy eigenvalues and can be tabulated for all  $\mathbf{p}$  and stored for future reference.

In our calculations for tungsten the interstitial part of the muffin-tin potential was expanded into 40 stars of plane waves. This "warped" muffin-tin potential is well suited for  $2\gamma$  momentum-distribution calculations in view of the preference of the positron for the interstitial region. A self-consistent electron potential was obtained in the local-density approximation and the eigenvalues were converged to within 0.2 mRy. Exchange and correlation effects were incorporated using the Hedin-Lundqvist scheme.<sup>14</sup> The contribution of the core states to the charge density was calculated in every iteration, properly taking into account the charge tails that extend into the interstitial region.<sup>15</sup> In the last few iterations an irreducible wedge of the Brillouin zone was sampled at 285  $\mathbf{k}$  vectors. The RLAPW expansion of the electron wave functions contained all reciprocal-lattice vectors with  $G < 3.74$  a.u., and the angular decomposition inside the spheres included all  $l \leq 8$ . A lattice parameter of 5.973 a.u. was used. The positron eigenvector was calculated using the electron potential after sign reversal and omission of the exchange-correlation part. All terms with  $l > 0$  together were found to contribute less than 1% to the total positron charge inside the muffin-tin sphere. Subsequently, the  $2\gamma$  momentum distribution was calculated for 24 000  $\mathbf{p}$  vectors in the  $\frac{1}{48}$ th irreducible wedge of momentum space within a radius of 4 a.u.

Figure 1 shows the relativistic band structure along line  $\Gamma H$ . For the purpose of comparison the inset shows the corresponding semirelativistic bands calculated by Jansen and Freeman.<sup>16</sup> In the semirelativistic calculation three bands cross the Fermi level, one of which is doubly degenerate. The spin-orbit interaction lifts this degeneracy and three bands appear with  $\Delta_7$  symmetry (the labels in Fig. 1 distinguish bands of the same symmetry by their superscripts). Their mutual repulsion creates a small energy gap at the Fermi energy. The  $\Delta_7$  bands, due to the symmetry of their wave functions, do not contribute to the  $2\gamma$  momentum distribution for momenta along the  $\langle 100 \rangle$  direction.<sup>17</sup> Therefore, the Lock-Crisp-West (LCW) theorem<sup>18,19</sup> is used. In its three-dimensional form the LCW procedure sums the  $2\gamma$  momentum distri-

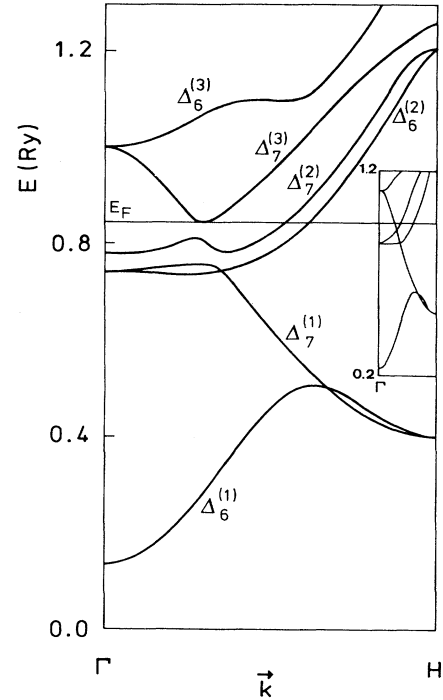


FIG. 1. The band structure of tungsten along line  $\Gamma H$ . The double-group symmetry notation is used to label the bands. The inset shows the corresponding semirelativistic energy bands (from Ref. 16).

bution for all momenta  $\mathbf{p}$  that can be reduced to the same wave vector  $\mathbf{k}$  by addition of a vector  $\mathbf{K}$  of the reciprocal lattice

$$h(\mathbf{k}) = \sum_{\mathbf{K}} \rho_{2\gamma}(\mathbf{k} + \mathbf{K}). \quad (23)$$

In the approximation of a constant positron wave function

$$h(\mathbf{k}) \approx \sum_n f_n(\mathbf{k}),$$

by wave-function normalization. For a realistic positron wave function the effect of the LCW procedure is to diminish the influence of the overlap integral  $A_n(\mathbf{p}, \mathbf{k})$ , so that the remaining structure in  $h(\mathbf{k})$  is predominantly caused by the occupation function  $f_n(\mathbf{k})$ , i.e., it reflects the Fermi surface. Please note that the inhomogeneity of the positron distribution is not the only reason that the LCW distribution deviates from the number of occupied bands. Although the contribution of the small electron components to the overlap integral is reduced through multiplication with the small positron components in Eq. (5) (for this reason it was neglected in our calculations), they do contribute in a non-negligible manner to the normalization of the electron wave function in a heavy-atom solid. However, the reduction of the LCW distribution due to this effect is generally small compared with the reduction caused by the inhomogeneity of the large positron components.

The influence of the overlap integral of band  $n$  is readi-

ly shown by application of the LCW procedure to  $|A_n(\mathbf{p}, \mathbf{k})|^2$ . Figure 2 shows the result of the "LCW folding." Large discontinuities arise where the bands  $\Delta_7^{(2)}$  and  $\Delta_6^{(2)}$  cross the Fermi level. In addition, a third feature can be seen, the origin of which lies in the contributions to  $h(\mathbf{k})$  of the  $\Delta_7$  bands. The Fermi level lies in the energy gap between  $\Delta_7^{(2)}$  and  $\Delta_7^{(3)}$ . The difference in electron-positron wave-function overlap for the states in the three bands results in an apparent transfer of momentum density across the gap. Since the  $\Delta_7^{(3)}$  band is not occupied, a net effect is visible in the total momentum distribution at about 0.3 the way along line  $\Gamma H$ . Due to its significant amplitude it may be mistaken for a Fermi-surface discontinuity in a 2D-ACAR experiment, but in reality it is a combined effect of the strong hybridization of the  $\Delta_7$  bands and the inhomogeneity of the positron distribution.

The present results can be compared to those of nonrelativistic momentum-distribution calculations by Singh and Singru<sup>20</sup> on isoelectronic Cr, the band structure of which closely resembles the results of the semirelativistic calculations on W shown in the inset in Fig. 1. In Cr the two bands which cross just below the Fermi level display rather flat contributions to the folded momentum distribution along line  $\Gamma H$  (Fig. 2 of Ref. 20). Their amplitudes differ by roughly 25%, which causes the same increase in the folded momentum distribution as in Fig. 2, in addition to a maximum in the small interval of momentum in which these two bands are both occupied.

## V. CONCLUSIONS

In this paper we have described a method to calculate the  $2\gamma$  momentum distribution using fully relativistic wave functions. An approximate expression, equivalent to the customary nonrelativistic expression, was used to calculate the overlap of the positron and electron wave functions; the Fermi surface, however, is determined by the fully relativistic band-structure calculation and enters the  $2\gamma$  momentum distribution through the Fermi-Dirac distribution function. Although the present method facilitates the interpretation of measurements on heavy-atom solids, a fully relativistic treatment of the overlap integral remains desirable.

Illustrative calculations on tungsten clearly show how the spin-orbit coupling may affect the Fermi surface and, consequently, the  $2\gamma$  momentum distribution.

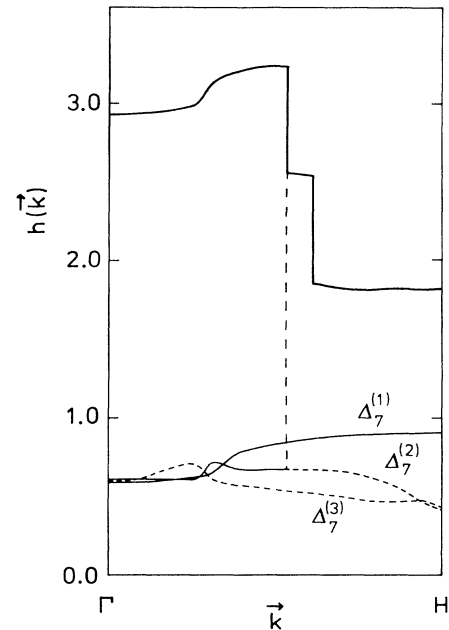


FIG. 2. The folded  $2\gamma$  momentum distribution along the  $\langle 100 \rangle$  direction. The momentum distributions of the individual  $\Delta_7$  bands are also shown. A dashed curve denotes empty  $\mathbf{k}$  states. The second Fermi-surface discontinuity is caused by band  $\Delta_6^{(2)}$ .

## ACKNOWLEDGMENTS

We would like to thank Dr. D. D. Koelling for many valuable discussions. One of the authors (G.J.R.) would like to thank Argonne National Laboratory for its hospitality. We acknowledge critical reading of the manuscript by Professor P. F. de Châtel and computing assistance by A. F. J. Melis. Work at Petten is part of the research program of the Stichting Fundamenteel Onderzoek der Materie (Foundation for Fundamental Research on Matter) and was made possible by financial support from the Nederlandse Organisatie voor Wetenschappelijk Onderzoek (Netherlands Organization for the Advancement of Research). The supercomputer time was financed by the National Fonds Gebruik Supercomputers (NFS) via the Foundation SURF. Work at Argonne was supported by the U.S. Department of Energy, Basic Energy Sciences—Materials Sciences, under Contract No. W-31-109-ENG-38.

<sup>1</sup>See references in *Positron Annihilation*, edited by L. Dorikens, M. Dorikens, and D. Segers (World Scientific, Singapore, 1989).

<sup>2</sup>See references in *J. Magn. Magn. Mater.* **76–77**, (1988).

<sup>3</sup>For instance, see S. DeBenedetti, *Nuclear Interactions* (Wiley, New York, 1964), pp. 416–419.

<sup>4</sup>V. Devanathan and K. Iyakutti, *J. Madras Univ. B* **45**, 188 (1982).

<sup>5</sup>For instance, see D. M. Bylander and L. Kleinman, *Phys. Rev. B* **29**, 1534 (1984).

<sup>6</sup>S. DeBenedetti, C. E. Cowan, W. R. Konneker, and H. Primakoff, *Phys. Rev.* **77**, 205 (1950).

<sup>7</sup>T. Takeda, *J. Phys. F* **9**, 815 (1979).

<sup>8</sup>M. E. Rose, *Relativistic Electron Theory* (Wiley, New York, 1961).

<sup>9</sup>K. Iyakutti and V. Devanathan, *J. Phys. C* **10**, 825 (1977).

<sup>10</sup>See, for example, W. Jones and N. H. March, *Theoretical Solid State Physics* (Wiley, London, 1973), Vol. 1, p. 93.

<sup>11</sup>T. L. Loucks, *Phys. Rev.* **139**, A1333 (1965).

<sup>12</sup>R. P. Gupta and R. W. Siegel, *Phys. Rev. B* **22**, 4572 (1980).

- <sup>13</sup>A. J. Arko and D. D. Koelling, *Phys. Rev. B* **17**, 3104 (1978).  
Here its quaternion reformulation was adopted: J. J. Dongarra, J. R. Gabriel, D. D. Koelling, and J. H. Wilkinson, *J. Comput. Phys.* **54**, 278 (1984).
- <sup>14</sup>L. Hedin and B. J. Lundqvist, *J. Phys. C* **4**, 2064 (1971).
- <sup>15</sup>D. D. Koelling, *Solid State Commun.* **53**, 1019 (1985).
- <sup>16</sup>H. J. F. Jansen and A. J. Freeman, *Phys. Rev. B* **30**, 561 (1984).
- <sup>17</sup>R. Harthoorn and P. E. Mijndarends, *J. Phys. F* **8**, 1147 (1978).
- <sup>18</sup>D. G. Lock, V. H. C. Crisp, and R. N. West, *J. Phys. F* **3**, 561 (1973).
- <sup>19</sup>S. Berko, in *Positron Solid-State Physics*, edited by W. Brandt and A. Dupasquier (North-Holland, Amsterdam, 1983), p. 64.
- <sup>20</sup>A. K. Singh and R. M. Singru, *J. Phys. F* **14**, 1751 (1984).